Sensitivity of liquid-state inherent structure to details of intermolecular forces

Frank H. Stillinger and Randall A. LaViolette
AT&T Bell Laboratories, Murray Hill, New Jersey 07974

(Received 19 August 1985; accepted 3 September 1985)

Temperature dependence of short-range order has been systematically studied in two model atomic liquids, using molecular dynamics computer simulation linked to steepest-descent mapping of configurations onto potential minima. Owing primarily to differing attractive forces, the natural crystal structures differ for the two models (face-centered-cubic vs primitive hexagonal). Only one of these crystals is geometrically consistent with the number of particles (256) and boundary conditions (periodic, cubic cell) used for both. Nevertheless, both liquids were found to exhibit temperature dependence of short-range order arising solely from vibrational smearing of underlying temperature-independent inherent structure. The latter differs substantially for the two models, and in each case resembles a highly defective version of the corresponding crystal.

I. INTRODUCTION

Recent theoretical and simulational studies of classical liquids have identified a useful simplifying principle, namely that at constant density they possess a temperature-independent inherent structure.[1–5] This principle is based upon a separation of the many-body problem into two parts.[6,7] The first consists in identifying and classifying the mechanically stable particle packings for the system of interest where each packing corresponds to a local minimum in the relevant potential energy function Φ. The second regards any arbitrary configuration of the particles as composed of a stable packing (identified by mass-weighted steepest descent on the Φ hypersurface) upon which has been imposed a "vibrational" deformation. Short-range order in the liquid under conventional conditions of thermal equilibrium reflects a combination of packing geometry and of vibrational distortion. Removing the latter strongly sharpens the image of short-range order which, by definition, then becomes the "inherent structure" for that liquid. Regions surrounding each of the Φ minima appear to be uniformly visited at and above the melting-point temperature T_m, and this fact underlies the temperature independence observed for the inherent structure.

But while any given model substance exhibits temperature-independent inherent structure, that inherent structure apparently can vary significantly according to the interactions that are present. Previous calculations of pair correlation functions for systems mapped onto potential minima seem to show quite distinct forms of short range inherent structure respectively for models of liquified noble gases,[1,2,8] molten alkali metals,[4,5] liquid silicon,[9] and metal-metalloid binary mixtures.[10,11]

Unfortunately this last conclusion, while reasonable, has been based upon a very heterogeneous group of computer simulations, involving different and small numbers of particles (108 to 216). The present paper was motivated by a desire to strengthen the above conclusion somewhat by comparing results for two different potentials, but with a common number of particles (256) and identical boundary conditions. The results confirm the previous thesis and broaden it to include a new class of inherent structure.

The following Sec. II defines the two models considered, one of which mimics the noble gases,[8] and the other of which at low temperature displays somewhat unusual crystallographic order.[12] Section III presents conventional pair correlation functions $g(r)$ for both models at several temperatures. Section IV shows corresponding results for the "quench pair correlation functions" $g_q(r)$ that result from removal of the vibrational deformation of the inherent structure. Conclusions are summarized in Sec. V.

II. PAIR POTENTIALS

Both cases to be considered involve pairwise additive central potentials:

$$\Phi(r_1 \cdots r_N) = \sum_{i<j} v(r_{ij}), \tag{2.1}$$

where the v's are selected from the family of functions ($a > 1$):

$$v(r) = A\,(r^{-p} - r^{-q})\exp[(r-a)^{-1}], \quad 0 < r < a$$
$$= 0, \quad a < r. \tag{2.2}$$

These are convenient for computer simulation applications because the interactions terminate at finite distance a, with all derivatives $v^{(n)}$ vanishing at that same point. Notice also that $v(1)$ vanishes.

Table I provides numerical values for the parameters A, p, q, and a for the two cases. In particular the first of these

TABLE I. Potential parameters.

	Case 1 ($v5$)	Case 2 (hx)
A	6.767 441	1.914 166
p	12	12
q	5	−3
a	2.464 918	2
r_m	1.122 462	1.348 077
Crystal form	fcc	primitive hex.
ρ_0	1.066 27	0.889 50
Φ_0/N	−7.162 077	−7.380 686

quantities has been selected to force the attractive well of v to have unit depth, which occurs at a pair separation

$$0 < r_m < a \tag{2.3}$$

that is also listed in Table I. We note that both cases have been recently examined[8,12] in somewhat different contexts.

Figure 1 shows the two pair potentials plotted together to contrast the distinct shapes that they possess. Case 1 (denoted below by $v5$) has much the narrower minimum, and in fact is a rather good match for the familiar Lennard-Jones 12-6 potential. However it is superior to the latter as a model for the noble gases (heavier than helium) in that it correctly yields the face-centered-cubic crystal as its lowest energy structure, while the Lennard-Jones 12-6 potential incorrectly yields the hexagonal close packed structure.[13] Case 2 (hx) utilizes its broader attractive well to cause the primitive hexagonal structure to be its lowest energy arrangement. This last feature is interesting in view of recent reports that solid silicon at high pressure transforms to the primitive hexagonal structure,[14,15] suggesting perhaps that the melt at this pressure may have a static local order similar to that of hx.

Table I also shows the values of the number density ρ_0 and of the lattice interaction energy per particle Φ_0/N for the zero-pressure, zero-temperature stable crystals.

III. CONVENTIONAL PAIR CORRELATIONS

Molecular dynamics simulations have been carried out for both pair potentials, using 256 particles, periodic boundary conditions, and cubic unit cells with respective sizes to produce the number densities ρ_0 listed in Table I. The standard fifth-order Gear algorithm[16] was used to integrate the Newtonian equations of motion. The number of particles and boundary conditions are concordant with formation of a perfect crystal (fcc) that is natural only for $v5$, not hx; consequently one of the goals of this study has been to see for the first time if "natural" vs "unnatural" boundary conditions might affect the existence of temperature-independent inherent structure in the liquid.

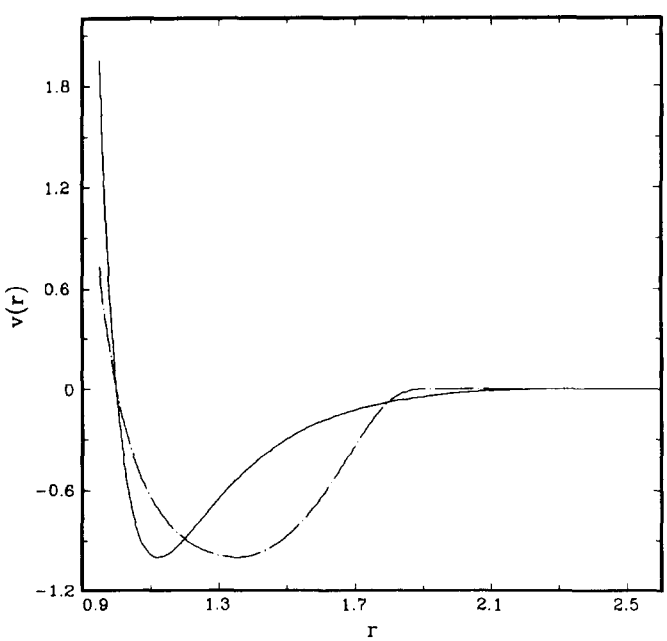

FIG. 1. Pair potentials for the two cases considered. The solid curve refers to $v5$, the broken curve to hx.

Table II lists the approximate freezing point temperatures T_f for the two cases, and the temperatures of the five states examined in the present study. Only two states were examined for $v5$, since (as remarked below) this case was found to conform closely to some similar models that have already been observed over a wide temperature range. Nevertheless, both a moderately supercooled state for $v5$ and an equilibrium hot liquid at more than twice the lower temperature were included for contrast. The less conventional hx was examined at three temperatures, all apparently in the thermodynamically stable liquid range, including one extremely high temperature which is approximately $160T_f$ for the model.

Time increments Δt for integration of the dynamical equations were selected to maintain to high accuracy constancy of total energy during runs. These increments typically were 0.001 25 for the low temperature liquids but had to be reduced for the higher temperature states. Well-equilibrated runs of at least 10^4 Δt were used to calculate pair correlation functions.

Figures 2 and 3 present the conventional pair correlation functions $g(r)$ that were determined for $v5$. They are similar to those that have been determined for other noble-gas models,[2] including that with the Lennard-Jones 12-6 pair potential.[17] The main point to notice is that the constant-density temperature rise between the states of Figs. 2 and 3 has caused a significant reduction in $g(r)$ peak heights and valley depths.

Figures 4, 5, and 6 display the analogous $g(r)$ results for hx, also in order of ascending temperature. It has been pointed out before[12] that the short-range order present in this model's liquid near the triple point is unusual. Specifically, the shoulder on the large-r side of the first $g(r)$ peak in Fig. 4 is never seen in other model liquids, and does not appear in the $v5$ results, Figs. 2 and 3.

When the temperature of the hx liquid rises to 2.08, Fig. 5, the prominent shoulder has virtually vanished. At the same time the distinctly asymmetric second $g(r)$ peak in Fig. 4 has, while diminishing in amplitude, become more nearly symmetrical. Rising temperature has evidently caused the hx liquid to transform short-range order in such a way that it more and more resembles the $v5$ model.

Figure 6 shows the $g(r)$ that results from extreme heating of the hx liquid. Only a very low first peak still persists, with no subsequent peaks or valleys perceptible over the statistical noise level. Particle collisions at this extreme temperature 84.8 are so energetic that the position of the remaining

TABLE II. Temperatures of thermodynamic states.

$v5$[a]	hx[b]
1.92	0.626
4.35	2.08
	84.8

[a] $T_f(v5) \cong 2.40$.
[b] $T_f(hx) \cong 0.53$.

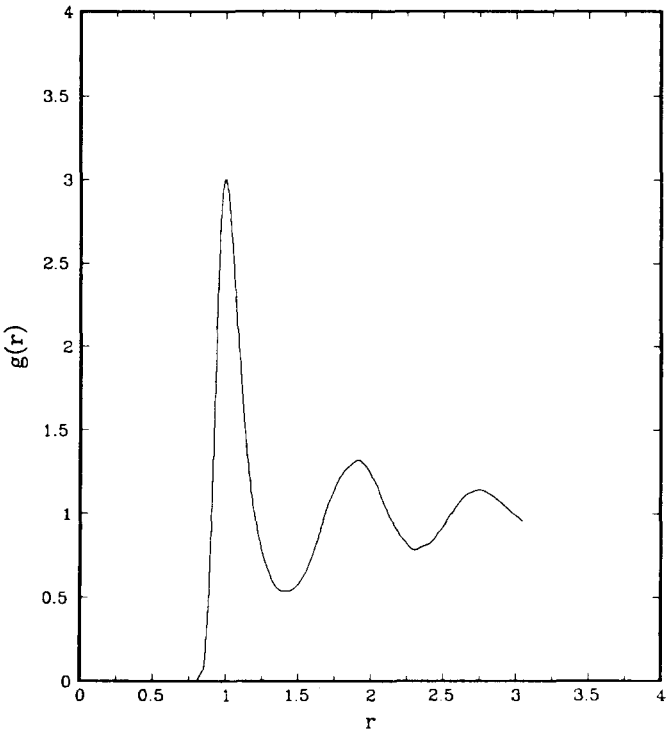

FIG. 2. Conventional pair correlation function for $v5$ at temperature 1.92, a supercooled liquid state.

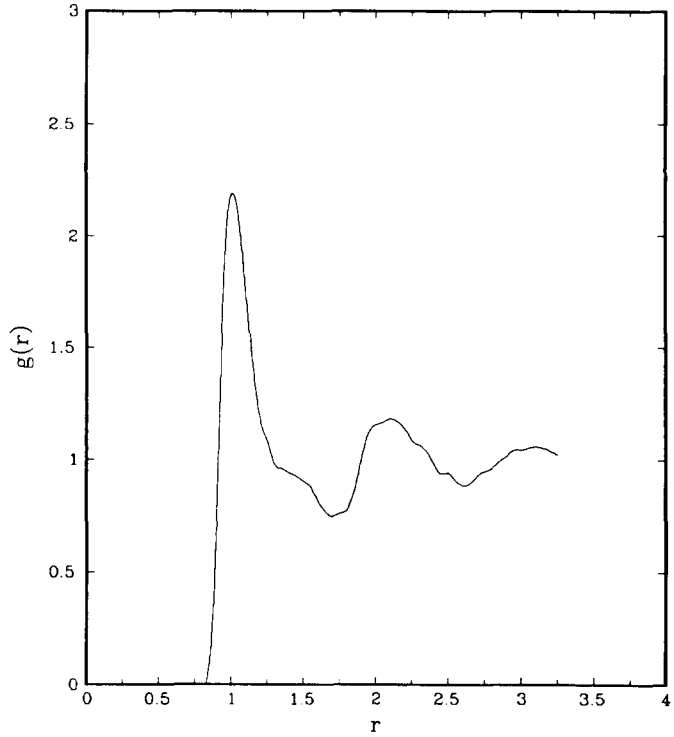

FIG. 4. Conventional pair correlation function for hx at temperature 0.626.

peak has been driven substantially inward to $r = 0.80 \pm 0.025$, compared to position $r = 0.95 \pm 0.025$ in Fig. 5 for temperature 2.08, and to $r = 1.00 \pm 0.025$ in Fig. 4 for temperature 0.626. At this high temperature extreme $g(r)$ is almost completely dominated by the repulsive part of the pair potential. A similar comment would also certainly apply to the $v5$ model in the same temperature regime. Since both $v5$ and hx have inverse-twelfth-power repulsive cores (Table I), it might therefore seem that both should exhibit a common inherent structure (namely that for the r^{-12} potential alone) when configurations are mapped from extreme high-temperature states to minima.

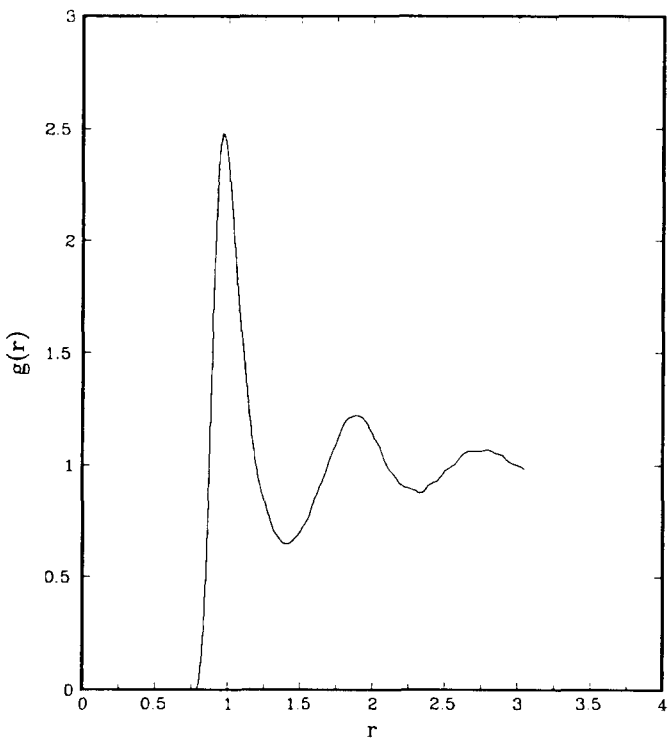

FIG. 3. Conventional pair correlation function for $v5$ at temperature 4.35.

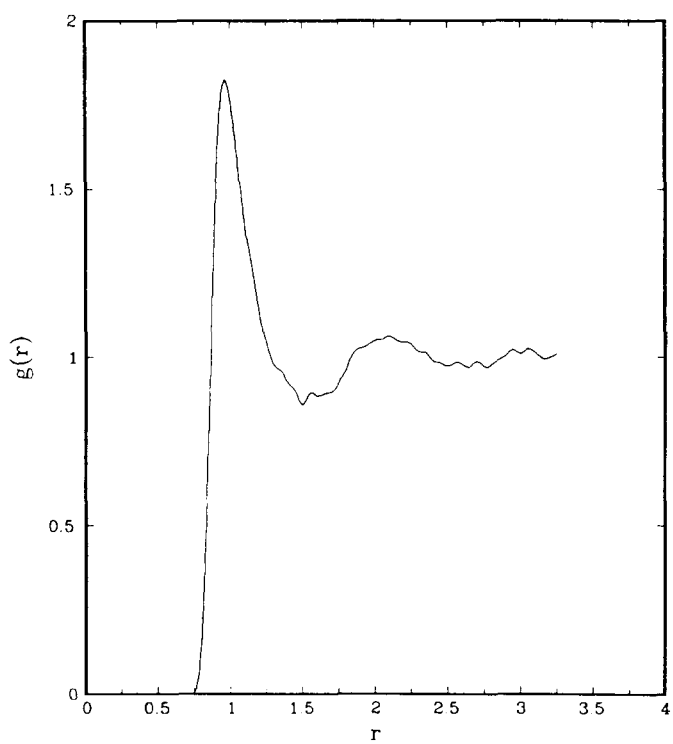

FIG. 5. Conventional pair correlation function for hx at temperature 2.08.

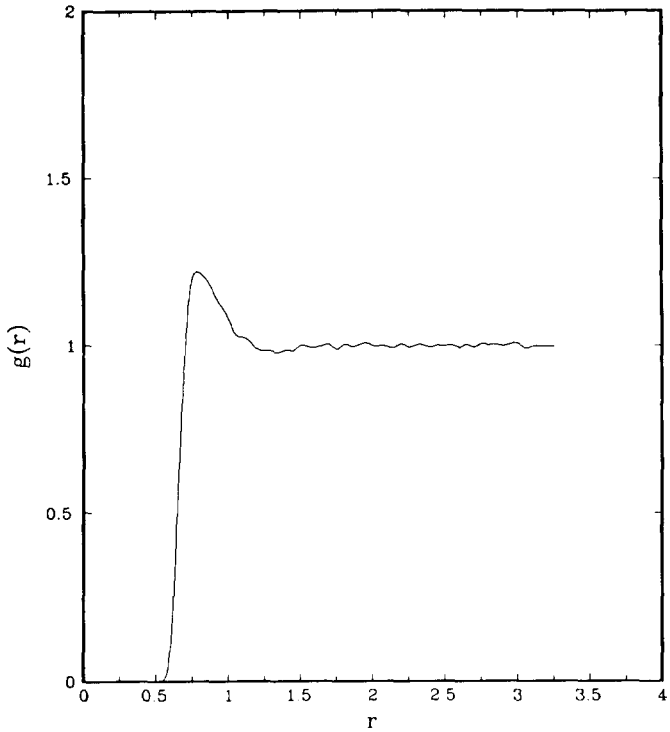

FIG. 6. Conventional pair correlation function for hx at temperature 84.8.

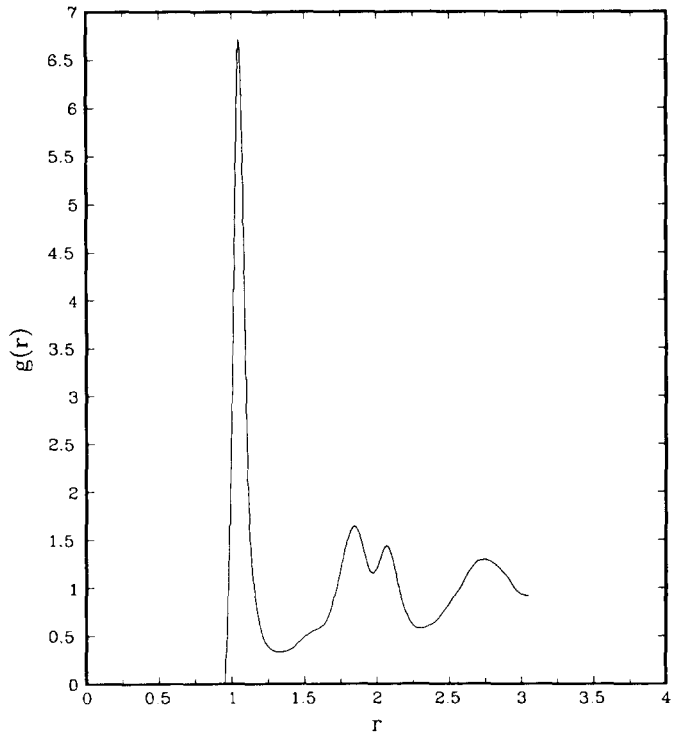

FIG. 7. Quench pair correlation function for $v5$, where the initial temperature was 1.92.

IV. QUENCH PAIR CORRELATION FUNCTIONS

At regularly spaced intervals during the five molecular dynamics runs, the digital computer was instructed to map the instantaneous configuration of the 256-particle system onto the relevant potential energy minimum. This operation produced a set of 100 "quenches" for each liquid state. These quenches were individually verified to be valid minima by calculating the eigenvalues of the force constant matrix and observing that all but the necessarily vanishing three were positive.

Quench pair correlation functions $g_q(r)$ were calculated as averages over the sets of 100 configurations at minima. By definition these are image-enhanced versions of the conventional $g(r)$ functions, created by removing vibrational deformation from configurations occurring along the dynamical trajectory. Examination of the sequences of potential energy values at the minima for $v5$ and hx runs seems to indicate that a representative sampling occurred for each state considered.

Figures 7 and 8 show $g_q(r)$ results for the two $v5$ states, and correspond respectively to the $g(r)$ curves in Figs. 2 and 3. Two features are clear. The first is that substantial sharpening has indeed occurred as a result of mapping to minima. The second is that within statistical sampling error to be expected with the relatively small number of configurations used, the $g_q(r)$ results are identical. This latter confirms once again that temperature variation of conventional pair correlation functions resides almost exclusively in the vibrational component, not in the atom-packing component.

Image enhancement for the $v5$ model resolves the second $g(r)$ peak into a three-component $g_q(r)$ feature. Two of these three components form a "split second peak" that has often been regarded as characteristic of the amorphous solid state.[18] It is important to notice that the three components have positions and magnitudes that suggest they are disrupted versions of second, third, and fourth neighbor shells in the face-centered-cubic lattice.[2,19]

Figures 9, 10, and 11 show quench pair correlation functions for hx, and correspond respectively to the earlier Figs.

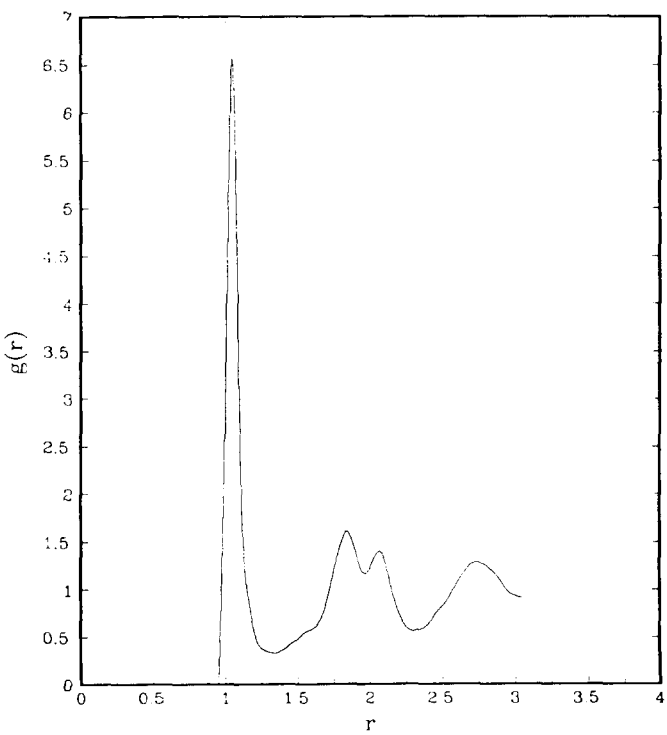

FIG. 8. Quench pair correlation function for $v5$, where the initial temperature was 4.35.

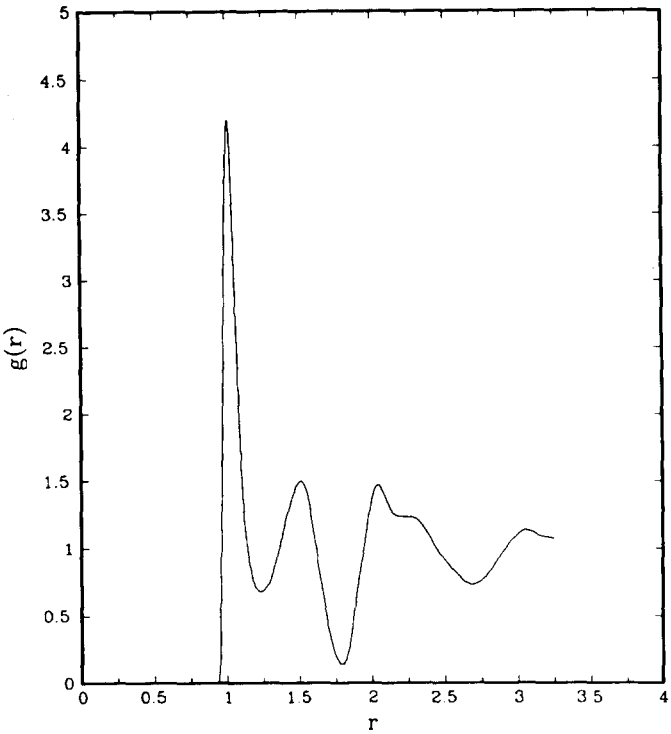

FIG. 9. Quench pair correlation function for hx, where the initial temperature was 0.626.

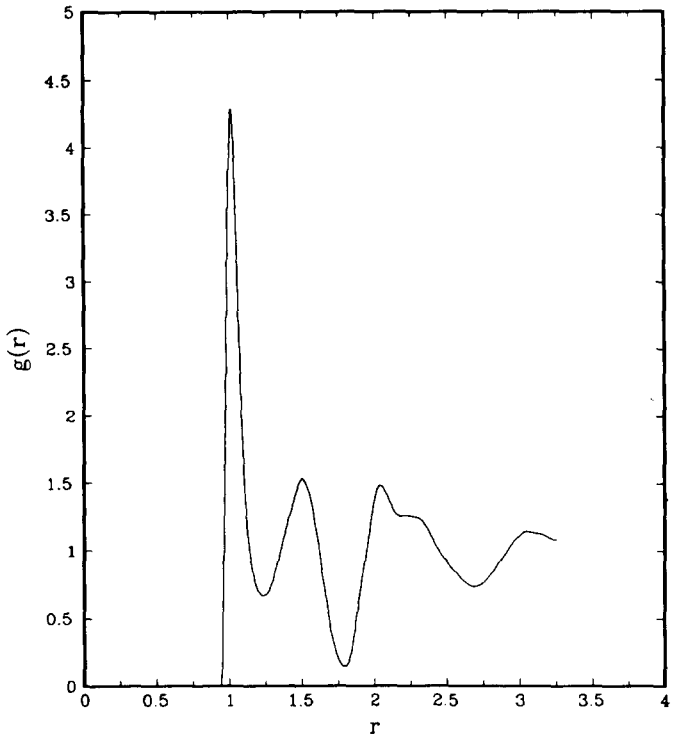

FIG. 11. Quench pair correlation function for hx, where the initial temperature was 84.8.

4, 5, and 6. Again the results demonstrate considerable image enhancement of the short-range order. Furthermore, they also agree with one another to within expected statistical uncertainty, and thus affirm that a temperature-independent inherent structure exists in the hx liquid as well. This conclusion is particularly vivid considering that the initial temperatures vary by a factor of 135, with widely differing $g(r)$ functions for the initial states. Even when the hx system starts at an extremely high temperature so that only repulsive core forces substantially influence $g(r)$, the mapping to potential minima causes the system to "remember" its full interaction.

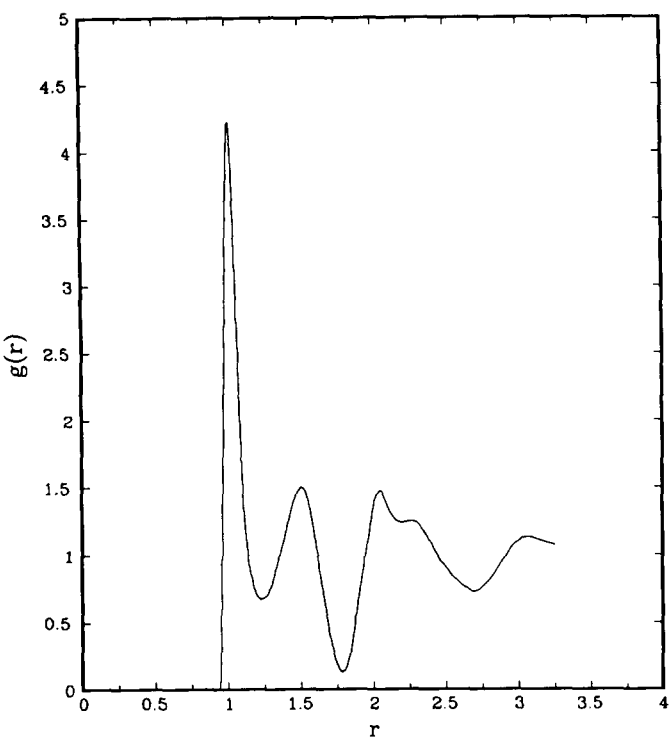

FIG. 10. Quench pair correlation function for hx, where the initial temperature was 2.08.

The temperature-independent inherent structures for $v5$ and for hx revealed by the respective g_q's are *not* the same. While both exhibit sharp first-neighbor peaks, those peaks display distinctly different heights. Furthermore the larger-distance features are significantly different for the two cases. The shoulder on the large-r side of the first $g(r)$ maximum for hx that is visible in Fig. 4 has developed in Fig. 9 to a well-resolved peak. The common function conveyed by Figs. 9–11 represents an amorphous packing, but without exhibiting the familiar "split second peak" of the type appearing in the $v5$ function. The $g_q(r)$ for hx can best be described as short-range order in a deformed and defective version of the simple hexagonal lattice.[12]

V. CONCLUSIONS

Pair correlation functions reported in this paper for both the $v5$ and hx models reinforce the earlier conclusion regarding temperature dependence of short-range order in the liquid phase. Specifically, when density is fixed, virtually all temperature dependence is attributable to the varying extent of vibrational excursions away from potential minima, provided that the temperature is not much below the thermodynamic freezing point T_f. Removal of the vibrational deformation is effected by the steepest-descent operation on the multidimensional potential energy hypersurface, with the result that the temperature-dependent conventional pair correlation functions $g(r, T)$ transform into temperature-in-

dependent quench pair correlation functions $g_q(r)$. This phenomenon of temperature independence emerges from the fact that liquids visit distinct regions surrounding potential minima with relative frequencies that do not vary substantially over the cited temperature range.

By implication analogous results should apply to higher-order correlation functions. The temperature dependence of nth order correlation functions $g^{(n)}(r_1 \cdots r_n, T)$ for $n > 2$ should likewise disappear under mapping to minima, leaving significantly image-enhanced quantities $g_q^{(n)}(r_1 \cdots r_n)$.

The best single indicator for the forms of the quench pair correlation functions $g_q(r)$ that are obtained from the liquid phase appears to be stable crystal structure for the given substance. Consequently the $g_q(r)$ results for $v5$ shown in Figs. 7 and 8 are closely similar to those for other models which also have the face-centered-cubic crystal as the structure of the absolute potential energy minimum, and furthermore the common $g_q(r)$ represents a defective face-centered-cubic particle packing. These other models include a shorter-range version of $v5$,[2] as well as inverse power potentials r^{-p} with $p = 12$ and 24.[20] Any change in the potential function that is sufficiently drastic to shift the absolute minimum structure to a different crystal type causes $g_q(r)$ thereupon to represent a defective version of that alternative crystal. The change in pair potential from the $v5$ model to the hx model illustrates this point quite clearly. Similarly, models whose crystals are body-centered-cubic[4,5] or which possess the tetrahedrally coordinated diamond structure[9] display their own characteristic $g_q(r)$ patterns.

The choice of cubic unit cell, periodic boundary conditions at the surface of that cell, and 256 particles for $v5$ are compatible with formation of that model's natural crystal (fcc) at low temperature, with no defects. The same choices were also exercised for the hx calculations, but are incompatible with formation of a defect-free simple hexagonal crystal. Nevertheless this incompatibility does not rule out the existence of a temperature-independent $g_q(r)$ for the hx liquid, evidently because it remains easy for the requisite highly defective packings of 256 particles to reside in the given periodic unit cell. We conclude that calculations of inherent short-range order in liquids is relatively insensitive to boundary conditions.

Substances which possess several crystalline modifications at ambient pressure deserve attention in future studies. It would be instructive to see which, if any, of those modifications correlate with the quench pair correlation functions. The group VI elements sulfur and selenium offer pertinent examples.[21] The first of these is particularly interesting in that it displays two isotropic liquids in different temperature ranges, separated by a critical anomaly[22]; this is surely a case which conventional liquid state theory is incapable of describing.[23] In view of the temperature-dependent chemical equilibria present in sulfur and in selenium between cyclic and linear polymeric atom groupings, unlike all cases heretofore examined, it may happen that quench pair correlation functions will show substantial dependence on initial-state temperature.

[1]T. A. Weber and F. H. Stillinger, J. Chem. Phys. **80**, 2742 (1984).
[2]F. H. Stillinger and T. A. Weber, J. Chem. Phys. **80**, 4434 (1984).
[3]F. H. Stillinger and T. A. Weber, Science **225**, 983 (1984).
[4]T. A. Weber and F. H. Stillinger, J. Chem. Phys. **81**, 5089 (1984).
[5]F. H. Stillinger and T. A. Weber, J. Chem. Phys. **81**, 5095 (1984).
[6]F. H. Stillinger and T. A. Weber, Phys. Rev. A **25**, 978 (1982).
[7]F. H. Stillinger and T. A. Weber, Phys. Rev. A **28**, 2408 (1983).
[8]R. A. LaViolette and F. H. Stillinger, J. Chem. Phys. **83**, 4079 (1985).
[9]F. H. Stillinger and T. A. Weber, Phys. Rev. B **31**, 5262 (1985).
[10]T. A. Weber and F. H. Stillinger, Phys. Rev. B **31**, 1954 (1985).
[11]T. A. Weber and F. H. Stillinger, Phys. Rev. B (to be published).
[12]R. A. LaViolette and F. H. Stillinger, J. Chem. Phys. **82**, 3335 (1985).
[13]J. O. Hirschfelder, C. F. Curtiss, and R. B. Bird, *Molecular Theory of Gases and Liquids* (Wiley, New York, 1954), p. 1041.
[14]H. Olijnyk, S. K. Sikka, and W. B. Holzapfel, Phys. Lett. A **103**, 137 (1984).
[15]J. Z. Hu and I. L. Spain, Solid State Commun. **51**, 263 (1984).
[16]C. W. Gear, *Numerical Initial-Value Problems in Ordinary Differential Equations* (Prentice-Hall, Englewood Cliffs, 1971).
[17]A. Rahman, Phys. Rev. A **2**, 405 (1964).
[18]G. S. Cargill, J. Appl. Phys. **41**, 12, 2248 (1970).
[19]F. F. Abraham, J. Chem. Phys. **72**, 359 (1980).
[20]F. H. Stillinger and T. A. Weber, J. Chem. Phys. **83**, 4767 (1985).
[21]J. Donohue, *The Structure of the Elements* (Wiley, New York, 1974), Chap. 9.
[22]*Elemental Sulfur*, edited by B. Meyer, (Wiley–Interscience, New York, 1965).
[23]D. Chandler, J. D. Weeks, and H. C. Andersen, Science **220**, 787 (1983).